Deep auscultation:
Predicting respiratory anomalies and diseases via recurrent neural networks

Diego Perna
DIMES - University of Calabria, Rende (CS), Italy
d.perna@dimes.unical.it

Andrea Tagarelli
DIMES - University of Calabria, Rende (CS), Italy
andrea.tagarelli@unical.it

Abstract

Respiratory diseases are among the most common causes of severe illness and death worldwide. Prevention and early diagnosis are essential to limit or even reverse the trend that characterizes the diffusion of such diseases. In this regard, the development of advanced computational tools for the analysis of respiratory auscultation sounds can become a game changer for detecting disease-related anomalies, or diseases themselves. In this work, we propose a novel learning framework for respiratory auscultation sound data. Our approach combines state-of-the-art feature extraction techniques and advanced deep-neural-network architectures. Remarkably, to the best of our knowledge, we are the first to model a recurrent-neural-network based learning framework to support the clinician in detecting respiratory diseases, at either level of abnormal sounds or pathology classes. Results obtained on the ICBHI benchmark dataset show that our approach outperforms competing methods on both anomaly-driven and pathology-driven prediction tasks, thus advancing the state-of-the-art in respiratory disease analysis.

1 Introduction

With the term "the Big Five", the World Health Organization identifies five respiratory diseases among the most common causes of severe illness and death worldwide, namely chronic obstructive pulmonary disease (COPD), asthma, acute lower respiratory tract infection (LRTI), tuberculosis, and lung cancer [1]. The number of people affected by COPD reaches 65 million, with about 3 million deaths per year, making it the third leading cause of death worldwide [2,3]. Asthma is a common chronic disease that is estimated

to affect as many as 339 million people worldwide [4], and it is considered the most common chronic childhood disease. Another widespread disease which especially affects children under 5 years old is pneumonia [5]. The *Mycobacterium tuberculosis* agent has infected over 10 million people, and it is considered the most common lethal infectious disease [6]. Yet, lung cancers kill around 1.6 million people every year [7].

Prevention, early diagnosis, and treatment are key factors to limit the spread of such diseases and their negative impact on the length and quality of life. Lung auscultation is an essential part of the respiratory examination and is helpful in diagnosing various disorders, such as *anomalies* that may occur in the form of abnormal sounds (e.g., *crackles* and *wheezes*) in the respiratory cycle. When performed through advanced computational methods, a deep analysis of such sounds can be of great support to the physician, which could result in enhanced detection of respiratory diseases.

In this context, *machine learning* techniques have shown to provide an invaluable computational tool for detecting disease-related anomalies in the early stages of a respiratory dysfunctions (e.g., [8–10]). In particular, *deep learning* (DL) based methods promise to support enhanced detection of respiratory diseases from auscultation sound data, given their well-recognized ability of learning complex non-linear functions from large, high-dimensional data. In recent years, this has led DL methods to set state-of-the-art performances in a wide range of domains, such as machine translation, image segmentation, speech and signal recognition.

In this work, we aim to advance the state-of-the-art in research on machine-learning detection of respiratory anomalies and diseases through the use of advanced DL architectures. A major contribution of our work is the definition of a learning framework based on *Recurrent Neural Network* (RNNs) models to effectively handle respiratory disease prediction problems at both anomaly- and pathology-levels. Unlike other types of DL networks, RNNs are designed to effectively discover the time-dependent patterns from sound data. To the best of our knowledge, the use of such models to address the above problems has not been adequately studied so far. We also contribute with a preprocessing methodology for a flexible extraction of core groups of cepstral features to feed the inputs to an RNN model. Remarkably, our RNN models were trained and tested using the *ICBHI Challenge* dataset, which provides an unprecedented, reproducible and standardized benchmark on which new algorithms can be fairly evaluated and compared [11]. Results obtained on the ICBHI benchmark, according to different assessment criteria, highlight the superiority of our RNN-based methods against all selected competitors that participated to the ICBHI Challenge, as well as against a further competitor based on a DL framework.

2 The ICBHI Challenge

The ICBHI Challenge dataset [11] was built in the context of a challenge on respiratory data analysis organized in conjunction with the 2017 Int. Conf. on Biomedical Health Informatics (ICBHI). The dataset contains audio samples that were collected independently by two research teams in two different countries. The data acquisition process was characterized by varying recording equipment, microphone chest position, environmental noise, etc. Such variability raised the level of difficulty of the challenge by introducing several sources of noise and unpredictability.

Annotations. The ICBHI sound data were provided with two types of annotation: i) for each respiratory cycle, whether or not crackles and/or wheezes are present, and ii) for every patient, whether or not a specific pathology from a set of predetermined categories is present. As we shall discuss in Sect. 3, all the participants to the ICBHI Challenge focused on the first, finer-grain type of annotations. To advance research on respiratory data analysis, in this work we also take the opportunity of exploiting the ICBHI Challenge to assess and comparatively evaluate our proposed framework on prediction tasks at either level of anomalies and pathologies.

2.1 Abnormal sounds

Crackles and wheezes are commonly referred to by domain experts as criteria to assess the health status of a patient's respiratory system. We adopt the definitions provided by The European Respiratory Society (ERS) on Respiratory Sounds and described in [12].

Crackles are discontinuous, explosive, and non-musical adventitious lung sounds, which are usually classified as *fine* or *coarse* crackles based on their duration, loudness, pitch, timing in the respiratory cycle, and relation to coughing and changing body position. The two types of crackles are normally distinguished based on their duration: longer than 10 ms for coarse crackles, and shorter than 10 ms for fine crackles. The frequency range of crackles is 60-2000 Hz, with most informative frequencies up to 1200 Hz [13].

Conversely, wheezes are high-pitched continuous, musical, and adventitious lung sounds, usually characterized by a dominant frequency of 400 Hz (or higher) and sinusoidal waveforms. Although the standard definition of continuous sound includes a duration longer than 250 ms, a wheeze does not necessarily extend beyond 250 ms and is usually longer than 80-100 ms. Severe obstruction of the intrathoracic lower airway or upper airway obstruction can be associated with inspiratory wheezes. Asthma and chronic obstructive pulmonary diseases (COPD) patients develop generalized airway obstruction. However, wheezing could even be detected in a healthy person towards the end of expiration after forceful expirations [13].
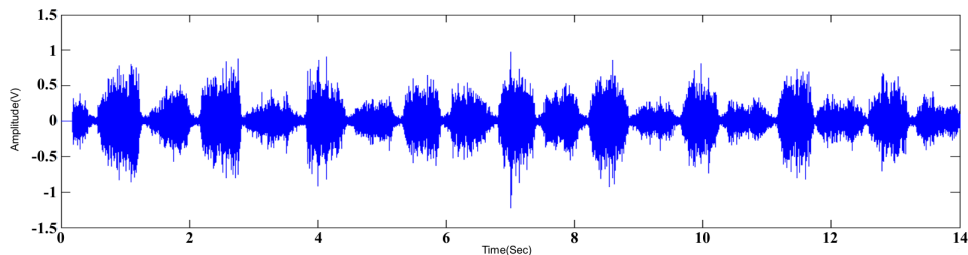
Figure 1: Example respiratory cycle waveform of a healthy patient.

2.2 Respiratory data

The ICBHI Challenge database consists of a total of 5.5 hours of recordings containing 6898 respiratory cycles, of which 1864 contain crackles, 886 contain wheezes, and 506 contain both crackles and wheezes, in 920 annotated audio samples from 126 subjects.

A single-channel respiratory sound, like the one shown in Figure 1, is composed of a certain number of cycles, which in turn include four main components, two pauses, and two distinctive patterns. Discarding fine-grain variations, mostly due to the conversion of air vibrations to electrical signal, a respiratory cycle is conventionally described as follows: it starts from the inspiratory phase, which is characterized by a lower amplitude and a regular pattern, then it follows with an expiratory phase, which shows one or multiple peaks, a decreasing amplitude pattern, and is usually characterized by a higher average energy.

As previously mentioned, the respiratory cycles were annotated by domain experts to state the presence of crackles, wheezes, a combination of them, or no adventitious respiratory sounds. More in detail, the annotation style format includes the beginning of the respiratory cycle(s), as well as the end of the respiratory cycle(s), the presence or absence of crackles, and the presence or absence of wheezes. The recordings were collected using heterogeneous equipment, with duration ranging from 10 s to 90 s. The average duration of a respiratory cycle is 2.7 s, with a standard deviation of about 1.17 s; the median duration is about 2.54 s, whereas the duration ranges from 0.2 s to above 16 s. Moreover, wheezes are characterized by an average duration of about 600 ms, with a relatively high variance, and a minimum and maximum duration value ranging between 26 ms and 19 s; conversely, crackles are characterized by an average duration of about 50 ms, smaller variance, and a minimum and maximum duration values of 3 ms and 4.88 s, respectively.

4

3   Related Work

We organize our discussion of related work into two parts, namely anomaly-driven prediction and pathology-driven prediction methods, depending on the target of classification of patients affected by respiratory diseases.

Anomaly-driven prediction.   In [8], the authors proposed a method based on hidden Markov models and Gaussian mixture models. The pre-processing phase includes a noise suppression step which relies on spectral subtraction [8]. The input of the model consists of Mel-frequency cepstral coefficients (MFCCs) extracted in the range between 50 Hz and 2,000 Hz in combination with their first derivatives. The method achieves performance results up to 39.37%, in compliance with the ICBHI score defined in [14]. The authors also tested an ensemble of 28 classifiers applying majority voting; this approach led to a slight improvement of the performance of a single classifier, though at the expense of ten times greater computational burden.

A method based on standard signal-processing techniques is described in [9]. The preprocessing phase here consists of a band-pass filter which is in charge of removing undesired frequencies due to heart sounds and other noise components. Then, the recording segment is separated into three channels, crackle, wheeze, and background noise, through resonance-based decomposition [15]. Subsequently, time-frequency and time-scale features are extracted by applying short-time Fourier transform to each individual channel. The resulting features are finally aggregated and fed into a support vector machine classifier. This method achieves 49.86% accuracy and an ICBHI score up to 69.27%.

The MNRNN method proposed in [10] is designed to perform end-to-end classification with minimal preprocessing needs. MNRNN consists of three main components: i) a noise classifier based on two-stacked recurrent neural networks which predicts noise label for every input frame, ii) an anomaly classifier, and iii) a mask mechanism which is in charge of selecting only noiseless frames to feed into the anomaly classifier. MNRNN achieves 85% accuracy in the detection of noisy frames, and ICBHI score of 65%.

The boosted decision tree model proposed in [16] utilizes two different types of features: MFCCs and low-level features extracted with the help of the *Essentia* library [17]. This method was mainly evaluated on a binary prediction setting (i.e., healthy or unhealthy), achieving accuracy up to 85%.

Pathology-driven prediction.   Differently from the above-mentioned methods, in our earlier work [18] we focused on the prediction task from the perspective of the pathology affecting the patient. Another key difference regards the input unit from which the coefficients have been extracted, which corresponds to a whole recording, rather than a respiratory cycle. The method in [18] is based on Convolutional Neural Networks (CNNs) and MFCCs coefficients, and exploits the class imbalance technique SMOTE.

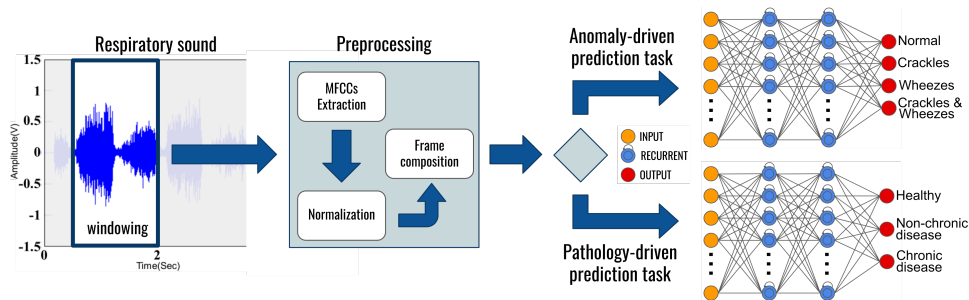In this work, we tackle the anomaly-driven prediction problem, as well

Figure 2: Illustration of our RNN-based framework for the prediction of respiratory anomalies and pathologies.

as the more challenging pathology-driven one. Similarly to [10], we define our method upon recurrent neural networks, but differently from it, we exploit the whole ICBHI dataset without omitting frames characterized by a high level of noise. In addition, like [8, 16, 18], our method also relies on MFCCs for the extraction of significant features from the respiratory sounds; however, the use of an RNN architecture allows our model to benefit from the discovery of time-dependent patterns, which otherwise would be ignored.

4   Our Proposed Learning Framework

In this section, we propose a novel framework which leverages on a particularly suitable type of deep neural network architecture, namely *recurrent neural networks* (RNNs). Unlike existing approaches, our framework is designed to handle a respiratory-disease prediction task at anomaly-level (*crackles* and *wheezes*) or at pathology-level — *chronic* diseases (COPD, bronchiectasis, asthma) and *non-chronic* diseases (Upper and Lower Respiratory Tract Infection (URTI and LRTI), pneumonia, and bronchiolitis) — at different resolutions (i.e., *two-class* or *multi-class* problems). Figure 2 provides a schematic illustration of the workflow of our framework. In the following, we motivate and describe the use of RNNs, then we discuss in detail the preprocessing phase, and the criteria used in our evaluation.

4.1   Recurrent Neural Networks

Traditional neural network architectures are based on the assumption that all inputs are sequentially independent. However, for many tasks, such as time-series analysis or natural language processing, in which the relations between consecutive training instances play a key role, this assumption is incorrect and could even be detrimental.

The basic idea behind RNNs is to enable a network to remember past data with the goal of developing better models by leveraging sequential in-

formation [19]. The term "recurrent" suggests that this type of architecture is characterized by repeatedly performing the same action to the input sequence. However, the key distinguishing feature of RNNs is that the output depends on the current input as well as on the previously processed samples. The ability of combining the informative content of the *i-th* sample and the previously processed ones can be ascribed as the capacity to "remember" a certain amount of samples back in time. In other words, RNNs can retain information about the past, enabling it to discover temporal correlations between events that are far away from each other in the data.

Early models of RNNs suffered from both *exploding and vanishing gradient* problems [20]. As advanced architectures of RNNs, *Long Short-Term Memory* (LSTM) and *Gated Recurrent Unit* (GRU) were designed to successfully address the gradient problems and emerged among the other architectures.

In this work, we profitably exploit the LSTM and GRU models in our prediction framework. Furthermore, we also employ the *bidirectional* version of both LSTM and GRU, dubbed BiLSTM and BiGRU, respectively, which differ from the unidirectional ones since they connect two hidden layers of opposite directions to the same output; in this way, the output layer can get information from past (backward) and future (forward) states simultaneously.

Setting. In both prediction tasks, we used the same configuration with 2 layers of 256 cells each with *tanh* activation function, under a Keras implementation on a Tensorflow backend.[1] To prevent overfitting, we introduced both regular and recurrent *dropout* [21]. In this regard, we tested different values for regular and recurrent dropout and found that the use of smaller values of recurrent dropout, w.r.t. the regular one, can lead to slightly better results. However, given the negligible nature of the performance improvement, we utilized the same value for both types of dropout, ranging between 30 and 60%. In addition, we leveraged the *batch normalization* [22] technique, with batch size equal to 32. Moreover, each of our RNN models was trained using the ADAM [23] optimization algorithm with start-learning rate set to 0.002. This is a computationally efficient technique for gradient-based optimization of stochastic objective functions, which has shown to be particularly useful when dealing with large datasets or high-dimensional parameter space. Finally, we set 100 training epochs for both the prediction tasks.

4.2 Preprocessing

We designed three steps of preprocessing of the ICBHI sound data: *frame composition*, *feature extraction*, and *feature normalization*. We elaborate on

---

[1] https://keras.io/, https://www.tensorflow.org/

Table 1: Configurations for the generation of RNN input frames from respiratory cycles

Setting id	Window size [ms]	Window step [ms]	#windows	Frame size [ms]	#features
S1	500	500	1	500	13
S2	500	250	1	500	13
S3	250	250	1	250	13
S4	50	50	5	250	65
S5	50	25	5	150	65
S6	50	50	10	500	130
S7	50	25	10	275	130

each of these steps next.

4.2.1 Frame composition

In the first step of our preprocessing scheme, we segment every respiratory cycle based on a sliding window of variable size, as described in Table 1. Subsequently, for each portion (i.e., window) of the respiratory cycle, we extract the Mel-Frequency Cepstral Coefficients (MFCCs) (cf. Sect. 4.2.2) and finally concatenate the coefficients of each window. The resulting group of cepstral features constitutes a *frame*, which represents the basic unit of data fed into the recurrent neural network.

As shown in Table 1, we devised 7 configurations by varying the size of the window, the step between consecutive windows, and the number of windows concatenated together after the extraction of the MFCCs. Note that the settings S1, S3, S4, and S6 are characterized by window size and window step of equal size, which results in a null overlap of two consecutive windows, and produces non-overlapping partitioning of the whole respiratory cycle. Conversely, the remaining settings correspond to a window step of half the size of the window, resulting in a 50% overlap between consecutive windows.

4.2.2 Feature extraction

For the extraction of significant features, we rely on Mel-Frequency Cepstral Coefficients (MFCCs) [24]. In speech recognition, MFCC model has been widely and successfully used thanks to its ability in representing the speech amplitude spectrum in a compact form.

In our framework, the extraction of MFCCs starts by dividing the input signal into frames of equal length and then applying a window function, such as the Hamming window to reduce spectral leakage. Next, for each frame, we generate a cepstral feature vector and apply the direct Fourier transform

(DFT). While information about the phase of the signal is discarded, the amplitude spectrum is retained and subject to logarithmic transformation, in order to mimic the way the human brain perceives the loudness of a sound [25]. Moreover, to smooth the spectrum and emphasize perceptually meaningful frequencies, we aggregate the spectral components into a lower number of frequency bins. Finally, we apply the discrete cosine transform (DCT) to decorrelate the filter bank coefficients and yield a compressed representation.

4.2.3 Feature normalization

Normalizing the input to a neural network is known to make training faster by limiting the chances of getting stuck in local minima (i.e., faster approaching to global minima at error surface) [26]. Within this view, we leverage two classic normalization techniques, Min-Max normalization and Z-score normalization (i.e., standardization). Recall that Z-score transformation of a feature value is calculated by subtracting the population mean by it and dividing this difference by the population standard deviation. Observed values above the mean have positive standard scores, while values below the mean have negative standard scores. By contrast, Min-Max normalization (i.e., subtracting the minimum of all values from each specific one and dividing the difference by the difference between maximum and minimum) scales feature values to a fixed range [0,1].

4.3 Evaluation and assessment criteria

For both prediction tasks under consideration, we divided the ICBHI dataset into 80% for training and 20% for testing. We used two groups of assessment criteria: i) ICBHI-specific criteria, based on *micro-averaging*, as required by the ICBHI Challenge, and ii) *macro-averaging* based criteria. The former group includes *sensitivity* and *specificity*, and their average, named *ICBHI-score*. Following the procedure described in [11, 14]:

$$Sensitivity = \frac{C_{crackles\_or\_wheezes}}{N_{crackles\_or\_wheezes}},$$

for the 2-class testbed,

$$Sensitivity = \frac{C_{crackles} + C_{wheezes} + C_{both}}{(N_{crackles} + N_{wheezes} + N_{both}},$$

for the 4-class testbed, and

$$Specificity = \frac{C_{normal}}{N_{normal}},$$

where Cs and Ns values denote the number of correctly recognized instances and the total number of instances, respectively, that belong to the class

crackles, *wheezes*, *both* (resp. *crackles_or_wheezes*), in the 4-class (resp. 2-class) testbed, or *normal*. Analogous definitions follow for the evaluation of pathology-driven prediction; for instance, in the 3-class testbed:

$$Sensitivity = \frac{C_{chronic} + C_{non\text{-}chronic}}{N_{chronic} + N_{non\text{-}chronic}}$$

$$Specificity = \frac{C_{healthy}}{N_{healthy}}.$$

We also considered macro-averaged *accuracy*, *precision*, *recall* (sensitivity), and *F1-score*, i.e., each of such scores is obtained as the average score over all classes. For instance, the 3-class pathology-driven evaluation accuracy is defined as:

$$Accuracy = \frac{1}{3}\left(\frac{C_{chronic}}{N_{chronic}} + \frac{C_{non\text{-}chronic}}{N_{non\text{-}chronic}} + \frac{C_{healthy}}{N_{healthy}}\right).$$

5   Experimental Results

Plan of experiments and goals.   We organize the presentation of experimental results into four sections, which correspond to our main goals of evaluation. First, we investigated the impact of feature normalization on the prediction performance of our framework (Sect. 5.1). Second, we compared the different types of RNNs considered in our framework, i.e., LSTM and GRU models, in their unidirectional and bidirectional architectures (Sect. 5.2). Third, we comparatively evaluated our approach to other methods in the context of the ICBHI Challenge, i.e., for the anomaly-driven prediction task (Sect. 5.3), and fourth, we conducted an analogous evaluation stage for the pathology-driven prediction task (Sect. 5.4).

5.1   Impact of feature normalization on RNN performance

We analyzed whether and to what extent normalization of the MFCC features is beneficial for the prediction performance of our framework. Table 2 reports accuracy results corresponding to the LSTM model, for various frame-composition settings, in the anomaly-driven prediction task, for both the binary testbed (i.e., presence/ absence of anomalies) and four-class testbed (i.e., normal, presence of crackles, presence of wheezes, presence of both anomalies).

Looking at the table, there is a clear evidence that the use of Z-score normalization generally leads to higher prediction accuracy, with significant improvements w.r.t. both min-max normalization and non-normalization of the features. This particularly holds for the four-class testbed.

Table 2: Accuracy performance by LSTM models in the anomaly-driven prediction task, for the binary and four-class testbeds.

Method	Un-normalized data		Min-Max Normalization		Z-score Normalization	
	2-Class	4-Class	2-Class	4-Class	2-Class	4-Class
LSTM-S1	0.74	0.69	0.68	0.64	0.78	0.72
LSTM-S2	0.75	0.67	0.68	0.68	0.77	0.73
LSTM-S3	0.75	0.69	0.73	0.68	**0.81**	**0.74**
LSTM-S4	0.76	**0.70**	0.77	**0.73**	0.79	**0.74**
LSTM-S5	0.77	0.69	**0.79**	0.72	0.79	0.72
LSTM-S6	**0.78**	0.68	0.77	0.70	0.77	0.73
LSTM-S7	0.76	**0.70**	0.79	0.72	0.80	0.72

The above finding was also confirmed by the other types of RNN used in our framework, with relative differences across the settings that revealed to be very similar to those observed for the LSTM model. For this reason, in the following we will present results corresponding to Z-score normalized features.

5.2 Comparison of RNN models

Figure 3 shows the accuracy obtained by the four different types of RNN models considered in our framework, i.e., LSTM, GRU, BiLSTM and Bi-GRU, for all frame-composition settings described in Table 1.

We observe that all architectures lead to relatively close performance, ranging between 0.70 and 0.74 across the different settings. Overall, the largest differences correspond to settings S4 and S1, whereby the BiLSTM model behaves alternately as the worst and the best solution, respectively. Also, the unidirectional GRU model tends to perform worse than the other models. In general, the LSTM models provide consistently better results in most cases, though at the expense of memory and training efficiency; in this regard, using the binary anomaly-driven prediction as a case in point, the time required to complete the training composed of 100 epochs was about 13 minutes for LSTM, 11 minutes for GRU, 26 minutes for BiLSTM, and 22 minutes for BiGRU.[2] Due to space limitations, in the following we will present results obtained by the use of the LSTM model in our framework.

5.3 Comparison with the ICBHI Challenge competitors

We compared our approach to methods that participated to the ICBHI Challenge (Sect. 3). In addition, we also included the CNN-based method in [18], which was not previously tested on the anomaly-driven prediction task.

---

[2]Experiments were carried out on a GNU/Linux (Mint 18) machine with Intel i7-3960X CPU and 64 GB RAM.
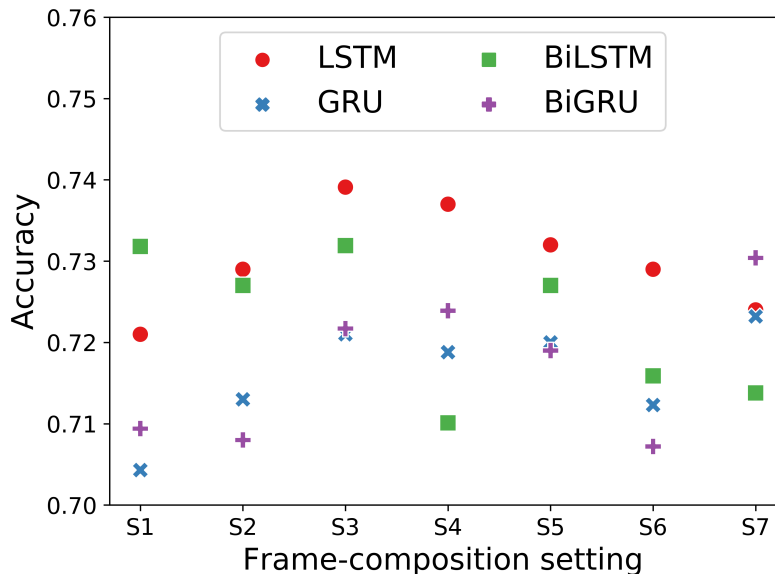
Figure 3: Comparison of RNN models in four-class anomaly-driven prediction

Table 3: ICBHI Challenge results on the detection of crackles and wheezes (four-class anomaly-driven prediction)

Method	Specificity	Sensitivity	ICBHI Score
Boosted Tree [16]	0.78	0.21	0.49
CNN [18]	0.77	0.45	0.61
HNN [8]	*na*	*na*	0.39
MNRNN [10]	0.74	0.56	0.65
STFT+Wavelet [9]	0.83	0.55	0.69
LSTM-S1	0.81	0.62	0.71
LSTM-S2	0.82	**0.64**	0.73
LSTM-S3	0.84	**0.64**	**0.74**
LSTM-S4	0.83	**0.64**	0.73
LSTM-S5	0.81	0.62	0.71
LSTM-S6	0.84	0.60	0.72
LSTM-S7	**0.85**	0.62	**0.74**

Results in Table 3 indicate that our LSTM models clearly outperfom all the competitors in terms of all three criteria. Note that the frame-composition settings that correspond to the best ICBHI-score in the challenge (i.e., 73%) are S2, S3 and S4, which are characterized by a different frame-size (i.e., 500, 250, and 50 ms), with total number of MFCCs equal to 13, 13, and 65, respectively. It should be noted that the relative difference in terms of ICBHI-score w.r.t. the other frame-composition settings is just 1-2%, which indicates robustness of our LSTM-based framework to a crucial step in the preprocessing of respiratory sound data.

Table 4: Performance of our LSTM-based methods vs. CNN-based method, in the pathology-driven classification tasks.

#classes	Method	Accuracy	Precision	Recall	F1-score	Specif.	Sensitiv.	ICBHI score
2	CNN [18]	0.83	**0.95**	0.83	0.88	0.78	0.97	0.88
2	LSTM-S1	0.98	0.92	0.85	0.88	0.70	**1.00**	0.85
2	LSTM-S3	0.98	0.93	0.87	0.89	0.77	0.99	0.88
2	LSTM-S4	**0.99**	**0.95**	**0.92**	**0.94**	0.79	**1.00**	0.89
2	LSTM-S6	0.98	0.92	0.88	0.90	0.80	0.99	0.90
2	LSTM-S7	**0.99**	0.94	0.91	0.92	**0.82**	0.99	**0.91**
3	CNN [18]	0.82	0.87	0.82	0.84	0.76	0.89	0.83
3	LSTM-S1	0.97	0.91	0.88	0.89	0.75	0.97	0.86
3	LSTM-S3	0.97	0.92	0.88	0.90	0.80	**0.98**	0.89
3	LSTM-S4	**0.98**	0.91	**0.90**	0.90	0.80	**0.98**	0.89
3	LSTM-S6	0.97	0.91	0.87	0.89	**0.82**	**0.98**	**0.90**
3	LSTM-S7	**0.98**	**0.93**	**0.90**	**0.91**	**0.82**	**0.98**	**0.90**

5.4 Performance on the pathology-driven prediction tasks

Table 4 summarizes performance results obtained by our LSTM-based framework against the CNN-based competitor [18] on the pathology-driven prediction task, in both binary (i.e., *healthy* or *unhealthy*) and ternary (i.e., *healthy*, *chronic*, or *non-chronic* diseases) fashion.

Looking at the results for the binary testbed, the best overall performance is achieved by our LSTM-based methods, in particular with frame-composition settings S4 and S7, which allow us to outperform the CNN-based method with gains up to 16% accuracy, 9% recall, 6% F1-score, 4% specificity, 3% sensitivity, and 3% ICBHI-score. The ternary testbed results strengthen the superiority of the LSTM-based methods vs. the CNN-based one, in all cases. Again, settings S7 and S4 lead to the best performance of our methods, which should be ascribed by the beneficial effect due to higher number of features and finer-grain windowing used to generate the RNN input frames.

6 Conclusion and Future Work

In this work, we developed a novel deep-learning framework that originally integrates MFCC-based preprocessing of sound data and advanced Recurrent Neural Network models for the detection of respiratory abnormal sounds (crackles and wheezes) and of chronic/non-chronic diseases. Our empirical findings, drawn from an extensive evaluation conducted on the ICBHI Challenge data and against different competitors, suggest that our RNN-based framework advances the state-of-the-art in two respiratory disease prediction tasks, i.e., at anomaly-level and pathology-level.

Our pointers for future research include the use or mixing of alternative DL architectures, and an investigation of the impact of alternative represen-

tation models for the respiratory sounds on the prediction performance of our framework. In particular, we are interested in developing hybrid models that can take advantage from a combination of time-series representation, whether in time or frequency domain, and MFCCs.

References

[1] "The global impact of respiratory disease (second edition)," *Forum of International Respiratory Societies*, 2017.

[2] A. A. Cruz, *Global surveillance, prevention and control of chronic respiratory diseases: a comprehensive approach.* WHO, 2007.

[3] P. G. Burney, J. Patel, R. Newson, C. Minelli, and M. Naghavi, "Global and regional trends in copd mortality, 1990–2010," *European Respiratory J.*, vol. 45, no. 5, pp. 1239–1247, 2015.

[4] "The global asthma report 2018," *Global Asthma Network*, 2018.

[5] T. Wardlaw, P. Salama, E. W. Johansson, and E. Mason, "Pneumonia: the leading killer of children," *The Lancet*, vol. 368, no. 9541, pp. 1048–1050, 2006.

[6] *World malaria report 2015.* World Health Organization, 2016.

[7] L. A. Torre, F. Bray, R. L. Siegel, J. Ferlay, J. Lortet-Tieulent, and A. Jemal, "Global cancer statistics, 2012," *Cancer journal for clinicians*, vol. 65, no. 2, pp. 87–108, 2015.

[8] M. Berouti, R. Schwartz, and J. Makhoul, "Enhancement of speech corrupted by acoustic noise," in *Proc. IEEE Int. Conf. on Acoustics, Speech, and Signal Processing*, vol. 4, pp. 208–211, 1979.

[9] G. Serbes, S. Ulukaya, and Y. P. Kahya, "An automated lung sound preprocessing and classification system based on spectral analysis methods," in *Precision Medicine Powered by pHealth and Connected Health*, pp. 45–49, Springer, 2018.

[10] K. Kochetov, E. Putin, M. Balashov, A. Filchenkov, and A. Shalyto, "Noise masking recurrent neural network for respiratory sound classification," in *Proc. Int. Conf. on Artificial Neural Networks*, pp. 208–217, 2018.

[11] B. Rocha, D. Filos, L. Mendes, I. Vogiatzis, E. Perantoni, E. Kaimakamis, P. Natsiavas, A. Oliveira, C. Jácome, A. Marques, *et al.*, "A respiratory sound database for the development of automated classification," in *Precision Medicine Powered by pHealth and Connected Health*, pp. 33–37, Springer, 2018.

[12] H. Pasterkamp, P. L. Brand, M. Everard, L. Garcia-Marcos, H. Melbye, and K. N. Priftis, "Towards the standardisation of lung sound nomenclature," *European Respiratory Journal*, vol. 47, no. 3, pp. 724–732, 2016.

[13] M. Sarkar, I. Madabhavi, N. Niranjan, and M. Dogra, "Auscultation of the respiratory system," *Annals of thoracic medicine*, vol. 10, no. 3, p. 158, 2015.

[14] N. Jakovljević and T. Lončar-Turukalo, "Hidden markov model based respiratory sound classification," in *Precision Medicine Powered by pHealth and Connected Health*, pp. 39–43, Springer, 2018.

[15] I. W. Selesnick, "Wavelet transform with tunable q-factor," *IEEE Trans. Signal Proces.*, vol. 59, no. 8, pp. 3560–3575, 2011.

[16] G. Chambres, P. Hanna, and M. Desainte-Catherine, "Automatic detection of patient with respiratory diseases using lung sound analysis," in *Proc. Int. Conf. on Content-Based Multimedia Indexing*, pp. 1–6, 2018.

[17] D. Bogdanov, N. Wack, E. Gómez, S. Gulati, P. Herrera, O. Mayor, G. Roma, J. Salamon, J. R. Zapata, and X. Serra, "Essentia: An audio analysis library for music information retrieval," in *Proc. Int. Soc. for Music Information Retrieval Conf.*, pp. 493–498, 2013.

[18] D. Perna, "Convolutional neural networks learning from respiratory data," in *Proc. IEEE Int. Conf. on Bioinformatics and Biomedicine*, pp. 2109–2113, 2018.

[19] I. J. Goodfellow, Y. Bengio, and A. C. Courville, *Deep Learning*. MIT Press, 2016.

[20] R. Pascanu, T. Mikolov, and Y. Bengio, "On the difficulty of training recurrent neural networks," in *Proc. Int. Conf. on Machine Learning*, pp. 1310–1318, 2013.

[21] Y. Gal and Z. Ghahramani, "A theoretically grounded application of dropout in recurrent neural networks," in *Proc. Int. Conf. on Neural Information Processing Systems*, pp. 1019–1027, 2016.

[22] C. Laurent, G. Pereyra, P. Brakel, Y. Zhang, and Y. Bengio, "Batch normalized recurrent neural networks," in *Procs IEEE Int. Conf. on Acoustics, Speech and Signal Processing*, pp. 2657–2661, 2016.

[23] D. Kinga and J. B. Adam, "A method for stochastic optimization," in *Proc. Int. Conf. on Learning Representations*, vol. 5, 2015.

[24] M. H. Shirali-Shahreza and S. Shirali-Shahreza, "Effect of mfcc normalization on vector quantization based speaker identification," in *Proc. IEEE Int. Conf. on Signal Processing and Information Technology*, pp. 250–253, 2010.

[25] S. Young, G. Evermann, M. Gales, T. Hain, D. Kershaw, X. Liu, G. Moore, J. Odell, D. Ollason, D. Povey, *et al.*, "The htk book," *Cambridge university engineering department*, vol. 3, p. 175, 2002.

[26] G. Montavon, G. B. Orr, and K. Müller, eds., *Neural Networks: Tricks of the Trade - Second Edition*, vol. 7700. Springer, 2012.